



ARL-TR-9099 • OCT 2020



Continuous Multihinged Composite for Exoskeletal Applications

by Colin Rowbottom and Daniel M Baechle

Approved for public release; distribution is unlimited.

NOTICES

Disclaimers

The findings in this report are not to be construed as an official Department of the Army position unless so designated by other authorized documents.

Citation of manufacturer's or trade names does not constitute an official endorsement or approval of the use thereof.

Destroy this report when it is no longer needed. Do not return it to the originator.



Continuous Multihinged Composite for Exoskeletal Applications

Colin Rowbottom

Oak Ridge Associated Universities, CCDC Army Research Laboratory

Daniel M Baechle

Weapons and Materials Research Directorate, CCDC Army Research Laboratory

REPORT DOCUMENTATION PAGE

*Form Approved
OMB No. 0704-0188*

Public reporting burden for this collection of information is estimated to average 1 hour per response, including the time for reviewing instructions, searching existing data sources, gathering and maintaining the data needed, and completing and reviewing the collection information. Send comments regarding this burden estimate or any other aspect of this collection of information, including suggestions for reducing the burden, to Department of Defense, Washington Headquarters Services, Directorate for Information Operations and Reports (0704-0188), 1215 Jefferson Davis Highway, Suite 1204, Arlington, VA 22202-4302. Respondents should be aware that notwithstanding any other provision of law, no person shall be subject to any penalty for failing to comply with a collection of information if it does not display a currently valid OMB control number.

PLEASE DO NOT RETURN YOUR FORM TO THE ABOVE ADDRESS.

1. REPORT DATE (DD-MM-YYYY) October 2020		2. REPORT TYPE Technical Report		3. DATES COVERED (From - To) 4 April 2019–17 September 2020	
4. TITLE AND SUBTITLE Continuous Multihinged Composite for Exoskeletal Applications				5a. CONTRACT NUMBER W911NF-18-2-0199	
				5b. GRANT NUMBER	
				5c. PROGRAM ELEMENT NUMBER	
6. AUTHOR(S) Colin Rowbottom and Daniel M Baechle				5d. PROJECT NUMBER	
				5e. TASK NUMBER	
				5f. WORK UNIT NUMBER	
7. PERFORMING ORGANIZATION NAME(S) AND ADDRESS(ES) CCDC Army Research Laboratory ATTN: FCDD-RLW-MA Aberdeen Proving Ground, MD 21005				8. PERFORMING ORGANIZATION REPORT NUMBER ARL-TR-9099	
9. SPONSORING/MONITORING AGENCY NAME(S) AND ADDRESS(ES) Oak Ridge Associated Universities 4692 Millennium Dr, Suite 101 Belcamp, MD 21017				10. SPONSOR/MONITOR'S ACRONYM(S)	
				11. SPONSOR/MONITOR'S REPORT NUMBER(S)	
12. DISTRIBUTION/AVAILABILITY STATEMENT Approved for public release; distribution is unlimited.					
13. SUPPLEMENTARY NOTES ORCID IDs: Colin Rowbottom, 0000-0001-8216-994X; Daniel M Baechle, 0000-0002-8875-8582					
14. ABSTRACT This report investigates a lightweight, continuous-fiber composite multihinged structure employing dual-matrix materials for tailorable torsional stiffness behavior with intended application for exoskeletons. Interfacing such a composite into exoskeletons requires a balance between optimizing torsional stiffness while allowing for localized out-of-plane bending, mimicking the flexibility and load-transfer capabilities of a human joint. Directional stiffnesses are optimized through the design analysis via Classical Laminate Theory. The composite-hinge layup consists of layers of continuous woven Kevlar fabric with alternating regions of epoxy and flexible polyurethane film and additional layers of woven carbon fabric in the epoxy sections to increase stiffness. This reports breaks up the design, fabrication, and testing of the composite-hinged samples into two sections. The first section investigates the effect that changes in hinge properties have on torsional stiffness for single-hinge composites. Low-cycle testing is used to evaluate the torsional stiffness of each design through a novel offset bend test in a load frame. The second section uses the single-hinge findings for design of multihinged composites for integration into an exoskeleton prototype. A comparison is made with an existing exoskeleton prototype comprising 2-D woven-carbon laminate plates connected to 1 degree-of-freedom aluminum hinges and steel hardware.					
15. SUBJECT TERMS high deformation, directional stiffness, exoskeletons, flexible composites, living hinges, vacuum-assisted resin transfer molding					
16. SECURITY CLASSIFICATION OF:			17. LIMITATION OF ABSTRACT UU	18. NUMBER OF PAGES 33	19a. NAME OF RESPONSIBLE PERSON Colin Rowbottom
a. REPORT Unclassified	b. ABSTRACT Unclassified	c. THIS PAGE Unclassified			19b. TELEPHONE NUMBER (Include area code) (410) 278-7634

Contents

List of Figures	iv
List of Tables	v
Acknowledgments	vi
1. Introduction	1
1.1 Motivation	1
1.2 Prior Work	2
1.3 Current Work and Applications	3
2. Experimentation	4
2.1 Design and Fabrication	4
2.2 Testing	9
3. Results	12
3.1 Single-Hinge Offset Bend Test	12
3.2 Multihinge Offset Bend Test	17
3.3 Exoskeletal Application	20
4. Conclusion	21
5. References	23
List of Symbols, Abbreviations, and Acronyms	24
Distribution List	25

List of Figures

Fig. 1	CCDC Army Research Laboratory’s Third Arm exoskeleton prototype	3
Fig. 2	Model of composite-hinge structure subjected to torsion and 3-D shear stiffness tensor state	5
Fig. 3	Composition of composite-fiber hinge structure segment	6
Fig. 4	Multihinge configuration	7
Fig. 5	Fabrication of composite-hinge structure: a, b) single-hinge and multihinge with PU strips; c, d) single-hinge and multihinge flanked by carbon sections; e, f) VARTM process; and g, h) post-cured composite, single and multihinge	8
Fig. 6	Representative fabricated composite-hinge samples: a) Designs 1–3, b) Design 4, c) Design 5, and d) Design 6	9
Fig. 7	Offset compression–bend test setup; left) carbon-fiber–Al hinge and right) dual-matrix composite-fiber hinge structure.....	10
Fig. 8	Free-body diagram of offset bend test; a) composite-hinge structure, b) rear, rigid carbon section, and c) free end subjected to load cell (coordinate system is with respect to the middle of the back panel) ..	10
Fig. 9	Experimental setup for multihinge offset bend test	11
Fig. 10	Torque vs. twist plots from offset bend test.....	13
Fig. 11	Average force threshold for each design	14
Fig. 12	Average torsional stiffness for each design	15
Fig. 13	Offset bend test’s progression for a) carbon–Al hinge and b) composite hinge.....	16
Fig. 14	Multihinge composite offset bend test’s results.....	18
Fig. 15	Multihinge offset bend test, force-deflection behavior of Trial 5 of Design 5	19
Fig. 16	Multihinge offset bend test, force-deflection behavior of Trial 5 of Design 6	20
Fig. 17	Integration of multihinge composite panel into Third Arm.....	21

List of Tables

Table 1	Fabric selection and properties	5
Table 2	Mechanical properties of fiber and matrix selection.....	5
Table 3	Design selections for composite single-hinge sections.....	6
Table 4	Design selections for composite multihinge sections	7
Table 5	Weight identification	12
Table 6	Weight selections for multihinge offset bend test.....	12
Table 7	Torsional stiffness for Designs 1–4 and Third Arm	15
Table 8	Comparison of masses of Third Arm and replacement multihinge composite panel	21

Acknowledgments

The authors would like to thank Mr Michael Thompson and Mr Michael Neblett for their assistance in composite fabrication and Mr David Gray for his assistance in mechanical testing. The authors would like to thank Mr Jim Wolbert for his assistance in composite fabrication and for his friendship and mentorship over the years; he is dearly missed. This research was sponsored by the US Army Combat Capabilities Development Command (CCDC) Army Research Laboratory (ARL) and was accomplished under Cooperative Agreement no. W911NF-18-2-0199. The views and conclusions contained in this document are those of the authors and should not be interpreted as representing the official policies, either expressed or implied, of CCDC ARL or the US government. The US government is authorized to reproduce and distribute reprints for government purposes notwithstanding any copyright notation herein.

1. Introduction

1.1 Motivation

Current robotic and human-scale exoskeletons have made significant advances over the years but the mechanical design of such systems still requires technological advancements. Most exo-suits and robotics remain rigid and bulky and present significant challenges for human-machine interface and energy-storage capabilities. Across industry, the US Department of Defense, and academia—each showing interest in designing and fabricating an efficient and effective system that is comfortable for the end user—such areas of focus shed light on reducing mass, parts, and, as a result, manufacturing and assembly labor. The design and analysis to reach this desired goal become convoluted when trying to match the motion of complex human joints and the energy-storage potential within muscle tissue during walking and running.

Generally, such systems will consist of a series of rigid members (“bones”) connected by single degree-of-freedom (DOF) metal hinges (“joints”) to produce the desired load-transfer pathway and appendage motion. These rigid members generally consist of lightweight metals such as aluminum (Al) or titanium or carbon-fiber composites that are as stiff and lightweight as possible to minimize the power and energy required to move them. To match the motion of the complexity of human joints, such as the shoulder or knee, often multiple 1-DOF metal hinges are used in series. These metal hinges can add significant bulk and mass to the exoskeleton or robot, and the interface between metal hinges and composite materials can be a point of failure. Misalignment of an exoskeleton’s hinges’ discrete center of rotation with the human joint’s complex and mobile center of rotation can cause discomfort for the wearer and reduce effectiveness of the device.

Composites with variable in-plane stiffness have the potential for tailorable hinge behavior in multiple-rotation axes by specifying ply and fiber orientation. Continuous composite hinges for exoskeletons could have multiple alternating rigid and flexible regions potentially alleviating functionality issues that arise from misalignment of human joints with metal hinges that have point centers of rotation. Such composite structures could provide a restorative or resistive force, eliminating the need for an external spring across a simple hinge, which could also reduce weight and improve efficiency of motion of human-scale exoskeletons.

1.2 Prior Work

The work presented in this report is a continuation of the work done by Rowbottom et al.¹ Prior to this, the main focus across academia and industry for dual-matrix composites was geared toward lightweight, foldable, deployable materials for outer-space structures. These foldable composite structures were designed for low-load applications and to be deployed once.

Sergio Pellegrino's group at the California Institute of Technology was successful in fabrication and testing of very thin dual-matrix continuous-fiber composites for foldable–deployable space structures.² They demonstrated the ability of the dual-matrix composite to fold once for storage and deploy once, further resisting bending and compression loads. Another work done by López and Pellegrino examined the folding of single-ply continuous carbon fibers in a silicone matrix.³ The authors used an unconventional compression–bend test to achieve high deformation in the material and through cyclic loading found evidence of damage though none was visible.

Platt's thesis details the fabrication and testing of woven carbon-fiber composites with alternating polyurethane (PU) and epoxy regions for the application of a folding tray table for passenger aircraft, and thus the composites were thicker than those for the deployable space structures.⁴ Samples were designed to resist loading under a constant-load 4-point bend test. Wet layup was performed by hand, which led to issues with porosity. Torsion properties were not evaluated.

Talon Technology has a commercially available dual-matrix continuous fiber carbon–Kevlar composite hinge consisting of rigid (epoxy matrix) outer wings and a flexible (urethane) unit.⁵ Due to their current design and fabrication process, the carbon–Kevlar hinge has a small radius of curvature, which limits the range of motion. This group performed high-cycle bend tests evaluating the stability of the flexible hinge unit as well as load strength. The results showed a slight reduction in the bending stiffness of the flexible hinge section. No other evidence of damage was shown. Torsional properties were not reported.

Rowbottom et al. demonstrated a novel method for manufacturing living hinges consisting of continuous-fiber woven composites of carbon fiber, Kevlar, epoxy, and PU with alternating epoxy (rigid) and PU (flexible) sections.¹ They demonstrated the ability to predict, design, and characterize torsional and flexural stiffness under low-cycle, high-deformation loading. This work opens up the possibilities to replace typical hinged-appendage assemblies in small robots, thus reducing the weight and complexity of the robot.

1.3 Current Work and Applications

In this report, the work done by Rowbottom et al.¹ on composite living hinges is extended to the application of high-load, human-scale exoskeletons. This work is broken up into two sections, first of which is the design, fabrication, and testing of dual-matrix composite living hinges. The torsional stiffness behavior is evaluated through a novel offset bend test, and Classical Laminate Theory (CLT) is used to predict the local effective torsional stiffness. The second section uses the findings from the first section to design, fabricate, and test dual-matrix multihinged composites for interfacing with the Third Arm exoskeleton prototype (Fig. 1).⁶

Third Arm was designed by the US Army Combat Capabilities Development Command (CCDC) Army Research Laboratory (ARL) and comprises a series of rigid, 2-D woven carbon-fiber laminate plates connected with steel fasteners to Al hinges. The Al hinges provide the stiffness necessary to support the load of weapons, shields, and tools weighing up to 13.6 kg (30 lb), while still allowing for smooth rotation and thus easy manipulation of the implement. However, the Al hinges and steel fasteners add weight and complexity to the overall device. The assembly of hinges and composite plates will be replaced by a single piece of composite with multiple alternating hinge and rigid sections. For such a composite to resist vertical load while allowing motion in the transverse plane about the body, there is a trade-off between maximizing torsional stiffness while still allowing for pliable out-of-plane bending through changes in number of plies, fiber orientation and overall width of the composite. The multihinged composite is interfaced with the Third Arm and a weight comparison is made with the original Al-hinge assembly.



Fig. 1 CCDC Army Research Laboratory's Third Arm exoskeleton prototype

2. Experimentation

2.1 Design and Fabrication

The design process of the composite living hinges is presented in detail in Rowbottom et al.¹ A numerical analysis to predict the torsional stiffness of the hinge was performed using CLT, where the composite is represented as an orthotropic angle-ply laminate with a rectangular cross section, based on the work done by Sumsion and Rajapakse.⁷ This approach is expressed in Equations 1–4, where w , t , and L_{eff} represent the width, thickness, and effective length of the flexible hinge region, shown in Fig. 2. In this model, the torsional stiffness, T/θ , is dependent on obtaining an accurate relation between the in-plane shear modulus, G_{xy} , and the out-of-plane shear modulus, G_{xz} . The in-plane shear modulus is obtained through Eq. 2 from CLT, where d_{ss} (sometimes written as d_{66}) is from the laminate compliance matrix.⁸ However, G_{xz} is difficult to predict without conducting experimental torsion tests about the fiber direction and transverse to the fiber direction, as described in the work of Tsai and Daniel.⁸ Evaluating Eq. 2 reveals the influence of laminate thickness: doubling the ply count results in approximately $2\times$ increase in G_{xy} . Davalos et al. reported that doubling ply count has a marginal effect on G_{xz} for orthotropic angle-ply laminates.⁹ Thus, for the purpose of this study a ratio of 0.01:1 ($G_{xz}:G_{xy}$) will be used for a single-ply composite hinge and 0.005:1 will be used for multi-ply composite hinges. The woven carbon fiber T300 was supplied by Toray and Kevlar S/4988 by Hexcel. The hinge's matrix material is a thin thermoplastic polyurethane film (TPU 399) supplied by Huntsman and the rigid epoxy system (SC-15) is supplied by Applied Pleramic, Inc. Figure 2 illustrates the composition of the composite-hinge structure where the outer regions are infused with SC-15 epoxy and the central hinge region uses a TPU thin film. SC-15 was chosen for its excellent mechanical properties and ease of processing using vacuum-assisted resin transfer molding (VARTM).

$$\frac{T}{\theta} = G_{xy} \left(\frac{wt^3}{L_{eff}} \right) \beta c \quad (1)$$

$$G_{xy} = \frac{12}{t^3 d_{ss}} \quad (2)$$

$$\beta = \frac{32c^2}{\pi^4} \sum_{n=1,3,5,\dots}^{\infty} \frac{1}{n^4} \left(1 - \frac{2c}{n\pi} \tanh \left(\frac{n\pi}{2c} \right) \right) \quad (3)$$

$$c = \frac{w}{t} \sqrt{\frac{G_{xz}}{G_{xy}}} \quad (4)$$

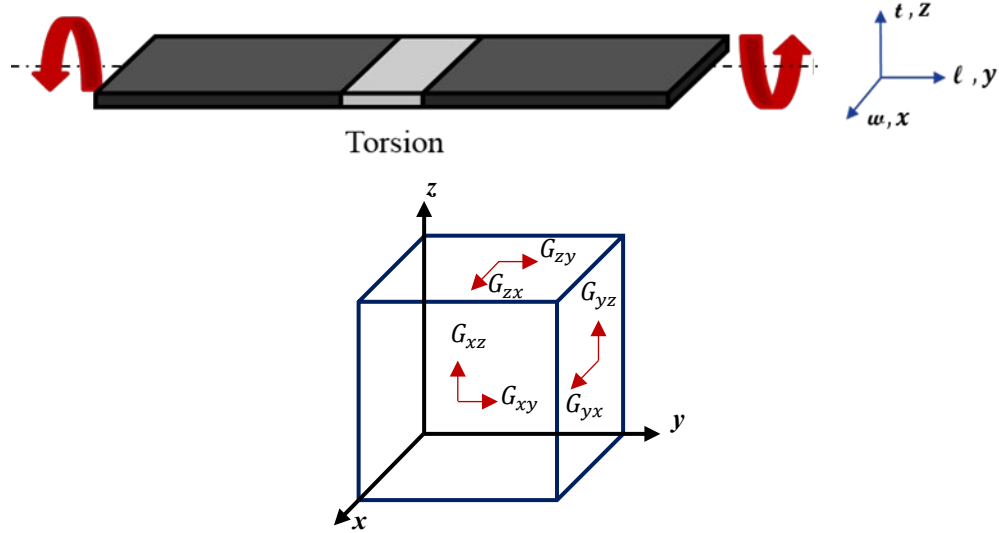


Fig. 2 Model of composite-hinge structure subjected to torsion and 3-D shear stiffness tensor state

The fiber and matrix selection along with the mechanical properties for the composite-hinge structures are listed in Tables 1 and 2.

Table 1 Fabric selection and properties

Fabric style	Carbon T300	Kevlar S/4988
Weight, g/m ²	197	508
Weave construction	Plain	8 × 8 Basket
Count, yarns/cm	4.72 × 4.72	15.7 × 15.7
Yarn type	3K Carbon	K49 1420 Denier

Table 2 Mechanical properties of fiber and matrix selection

Fiber properties	Carbon T300	Kevlar S/4988	Matrix properties	TPU 399	SC-15
E_{1f} (GPa)	230	131
E_{2f} (GPa)	15	7	E_m (MPa)	2.0	2500
G_{12f} (GPa)	27	21	G_m (MPa)	0.68	925
ν_{12}	0.20	0.33	ν_m	0.47	0.35

It is desirable to maximize composite torsional stiffness for integration of the composite-hinge structure into the Third Arm exoskeleton prototype; thus, the effects of changes in the number of plies and overall composite width are examined. The design selections for the single-hinge composite panels are outlined in

Table 3, which includes each selection’s length (L), width (W), and thickness (T). The length of the hinge section for each design case was chosen as 12.7 mm based on the findings reported by Rowbottom et al.¹

Table 3 Design selections for composite single-hinge sections

Design	Hinge fiber	Hinge matrix	Hinge fiber orientation	Hinge geometry L × W × T (mm)
1	Kevlar	PU 399	1 ply [±45]	12.7 × 152.4 × 1.5
2	Kevlar	PU 399	2 ply [±45]	12.7 × 152.4 × 2.8
3	Kevlar	PU 399	3 ply [±45]	12.7 × 152.4 × 3.2
4	Kevlar	PU 399	2 ply [±45]	12.7 × 76.2 × 2.3

For Designs 1–4, the fiber orientation of the rigid carbon sections are 4 ply [0°/90°] on top and bottom of the mid-plane Kevlar fibers (see Fig. 3). Single-hinge Designs 1–4 were fabricated and tested first to provide insight into the design composition of a multihinge composite structure.

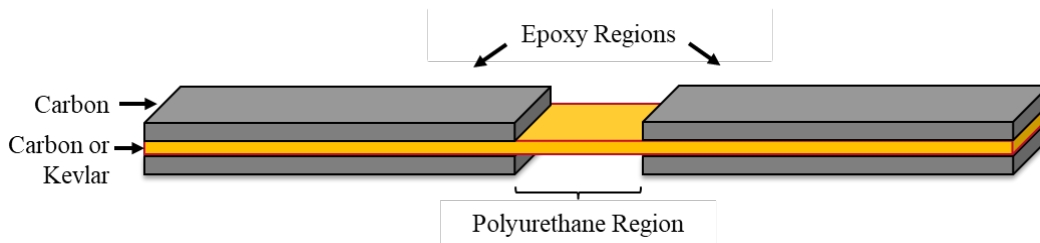


Fig. 3 Composition of composite-fiber hinge structure segment

The design selections for the multihinge composite are outlined in Table 4 and the geometry for each segment is illustrated in Fig. 4. The composition of each segment of the multihinge is the same as shown in Fig. 3 with alternating rigid and flexible regions. Note, however, that in Design 6 the carbon plies in each segment increases from right to left. The first two rigid segments have four carbon plies on each side of the Kevlar fabrics, the next segment has six carbon plies on each side, and the leftmost segment has eight carbon plies on each side of the Kevlar. The ply count was increased in the segments nearest the body to provide additional torsional stiffness in the sections that experience the highest torque due to the cantilever loading on the opposite end of the multihinge panel. The rear carbon-fiber-plate–Al hinge section of Third Arm will also be tested as a baseline for comparison with the living hinges. The 2-D woven carbon-fiber laminate plates used in this study have dimensions of 139.7 × 63.50 × 6.35 mm for the back plate and 244.50 × 63.50 × 6.35 mm for the following plate. The Al hinge is made from Al 6061-T6.

Table 4 Design selections for composite multihinge sections

Design	Hinge fiber orientation	Rigid fiber orientation	Hinge geometry L × W × T (mm)	Overall geometry L × W (mm)
5	3 ply [±45]	4 ply [0/90, ±45] _s	12.7 × 152.4 × 3.8	660.4 × 152.4
6	3 ply [±45]	8 ply [±45] _s ^a	12.7 × 101.6 × 3.9	660.4 × 101.6

^a Rigid fiber segments, ply count, from left to right in Fig. 4: 8, 6, 4, and 4

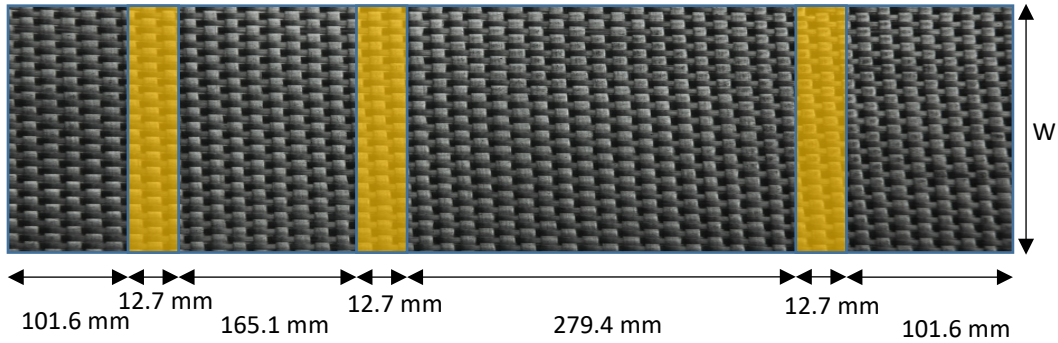


Fig. 4 Multihinge configuration

The panels were fabricated in a two-step process. PU films were first bonded to the flexible regions of the Kevlar in a vacuum-assisted autoclave process. Then, the flexible regions were masked with tape and the carbon fabrics laid in place. In the multihinge panels, orange 3-D-printed strips (Fig. 5D) were placed under the PU–Kevlar sections to maintain spacing of the carbon plies. The carbon fabrics and the unmasked Kevlar were then infused with epoxy using a VARTM process with an autoclave cure. (Further details of the fabrication process can be found in Rowbottom et al.¹) After autoclave cure, the panels were cut on a water jet to the sizes seen in Tables 3 and 4, and Figs. 5 and 6.

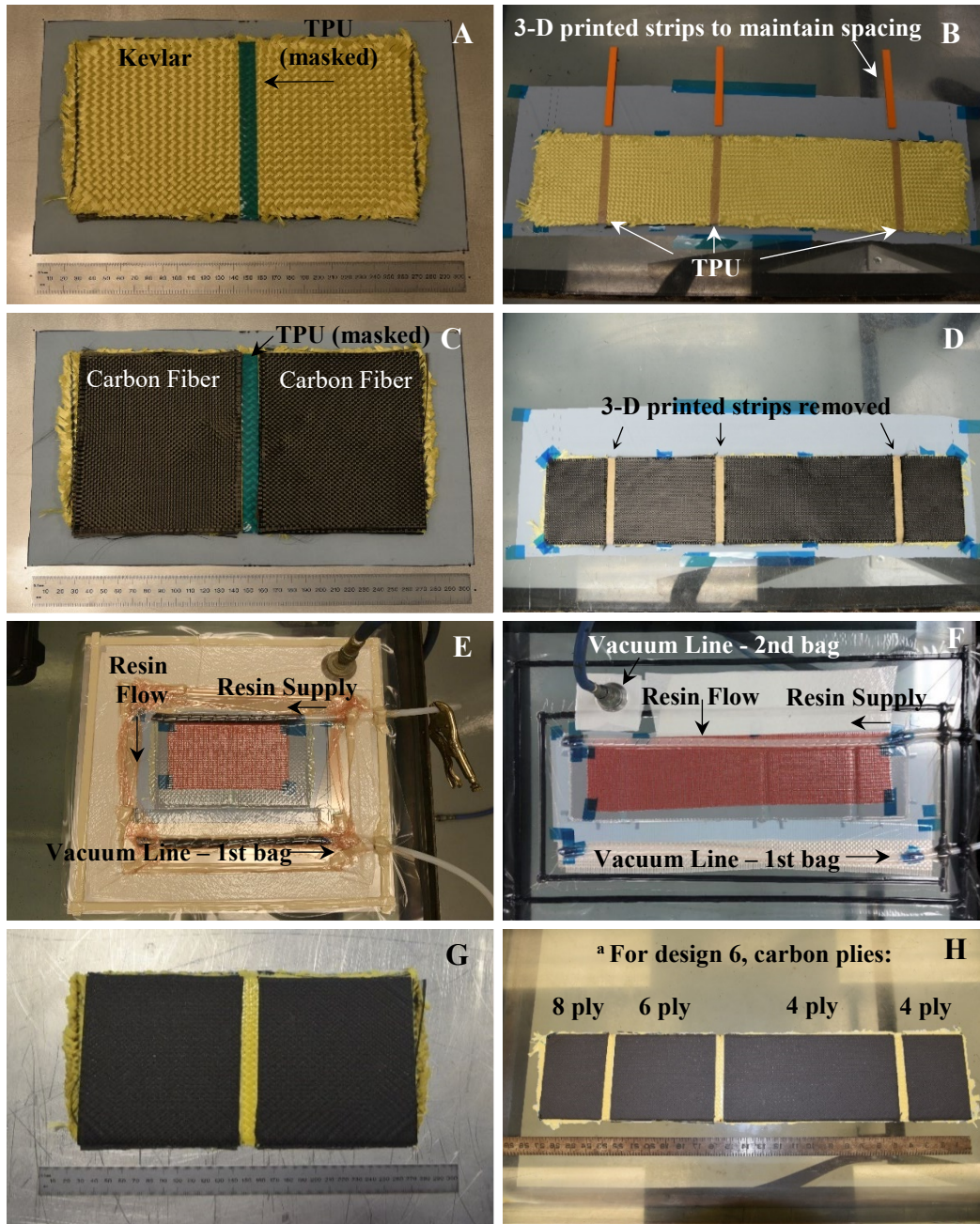


Fig. 5 Fabrication of composite-hinge structure: a, b) single-hinge and multi-hinge with PU strips; c, d) single-hinge and multi-hinge flanked by carbon sections; e, f) VARTM process; and g, h) post-cured composite, single and multi-hinge

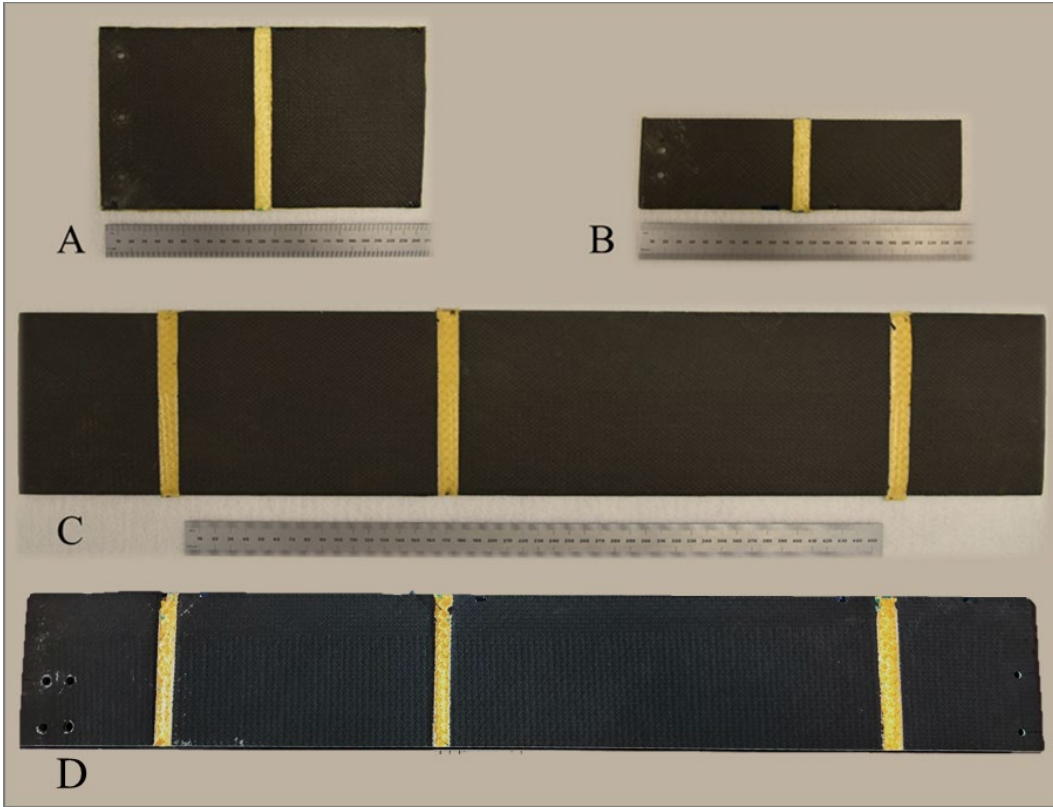


Fig. 6 Representative fabricated composite-hinge samples: a) Designs 1–3, b) Design 4, c) Design 5, and d) Design 6

2.2 Testing

The following tests were designed to evaluate the effectiveness of a composite-hinge structure to interface with the Third Arm exoskeleton prototype and replace its current 1-DOF carbon-fiber–Al hinge segments. The torsional stiffness is to be evaluated for both the single and multi-hinge panels through a novel offset bend test. The offset bend test replicates conditions in Third Arm for full-scale composites that will not fit in the available torsion-test frames. An Al test fixture was fabricated to hold the hinge structures at a 90° bend, with one end pinned and the other free (Fig. 7). A free-body diagram of the experiment is detailed in Fig. 8. As demonstrated previously,¹ some degree of damage occurs within the hinge section during the initial bending, but the hinge retains significant stiffness upon cyclic loading. A guided support was placed in parallel to the free end of hinge structure in order to keep the end aligned with the load cell. A strip of polytetrafluoroethylene (commonly, PTFE)-coated fiberglass adhesive film was placed on the guided support column to reduce sliding friction between the support column and the composite during testing. Testing was conducted on an Instron 5500R test frame with a 4448-N (1000-lb) load cell. A compressive load was

applied at the free end, 10 cm (4 inches) from the center of the hinge as shown in Fig. 7.

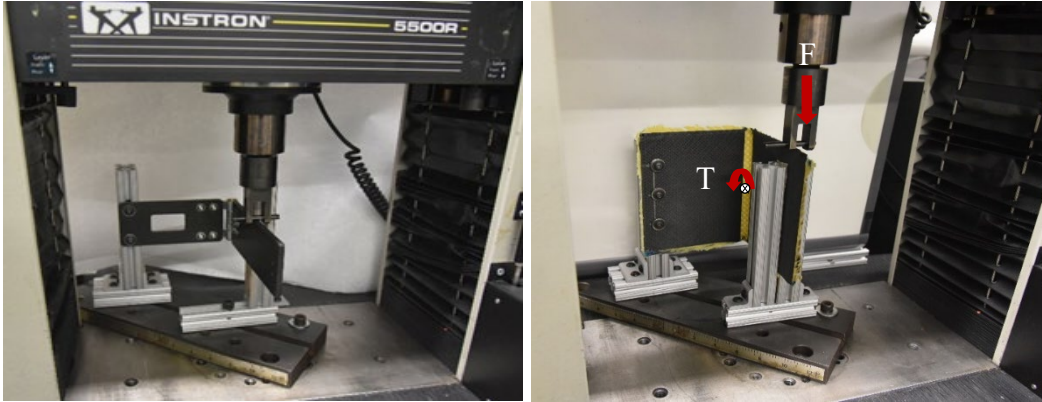


Fig. 7 Offset compression-bend test setup; left) carbon-fiber-Al hinge and right) dual-matrix composite-fiber hinge structure

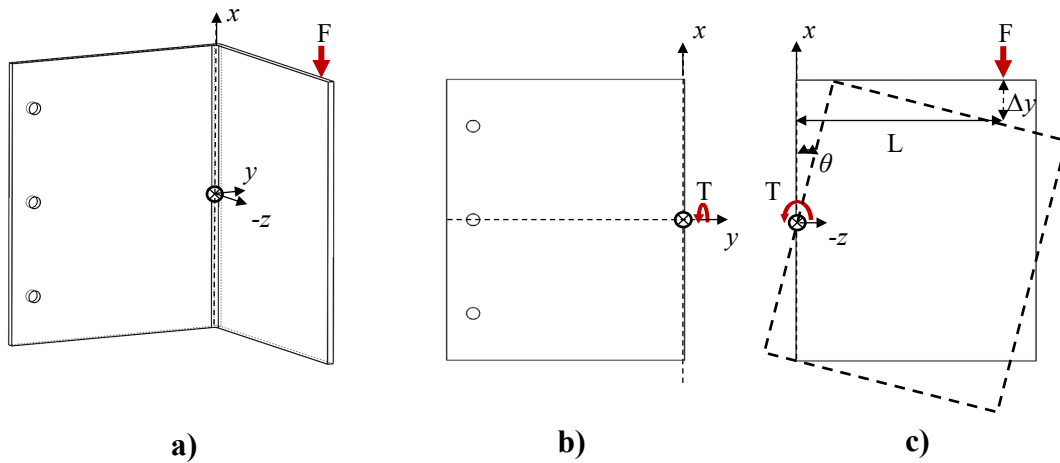


Fig. 8 Free-body diagram of offset bend test; a) composite-hinge structure, b) rear, rigid carbon section, and c) free end subjected to load cell (coordinate system is with respect to the middle of the back panel)

The rear carbon-fiber-Al hinge from the Third Arm as well as Designs 1–4 underwent a compressive load applied at a rate of 10 mm/min until a displacement of 25.4 mm was reached. Load application was repeated for five cycles, with a 5-min relaxation period between each cycle. Torsional load, T , in the hinge section was evaluated as the force applied by the load cell multiplied by the distance, L , of the “lever arm” to the center of the hinge. The assumption was made that the force applied from the load cell remains at distance L of 10 cm from the center of the hinge throughout the experiment. Torsional stiffness, T/θ , was evaluated at the center point of the hinge section and the angle of twist, θ , was derived through

geometric relations as described in Eq. 5, where Δy is the vertical displacement. This approximation likely does not capture the exact behavior of the composite hinge, but provides an application-relevant comparative metric between the composite-hinge designs and the Al hinge. At a minimum, the composite hinge should be able to withstand a torsional load of 37 Nm, which is equivalent to a 4.5-kg (10-lb) rifle fully supported by Third Arm in the most distal position. Ideally, the composite hinge would be able to withstand up to 112 Nm, which represents a 13.6-kg (30-lb) implement held at arm's length.

$$\theta = \tan^{-1} \left(\frac{\Delta y}{L} \right) \quad (5)$$

Testing of the continuous fiber multihinged composite panels were done in the same manner as the single-hinge offset bend test, but on a larger scale and without the use of a load frame. A simple Al test platform was designed for this experiment as shown in Fig. 9. As in the single-hinge bend test, one end is pinned to the test fixture and the rear hinge section is held in place at a 90° bend by a guided support. The free end was subjected to vertical loading through the use of a hanging dumbbell placed at a distance of 0.56 m (22.06 inches) from the center of the rear hinge. The selection of free-hanging weights used in this experiment are listed in Table 5. Each plate was weighed on a scale and recorded prior to testing. The combination of weights used for loading the multihinge are listed in Table 6. Trial 1 was meant to approximate the load of an M4 rifle, Trial 5 the load of an M249 machine gun, and Trial 6 the load of an M240B machine gun. For each applied weight, vertical deflection was recorded as well as experimental observations seen during testing of the composite hinge panels. The torsional stiffness behavior in the rear hinge section was evaluated the same way as in the single-hinge offset bend test. In addition, the multihinge composites were integrated into the Third Arm exoskeleton prototype (seen in Fig. 1) to replace the current carbon–Al hinge system. A weight comparison is presented in Section 3.

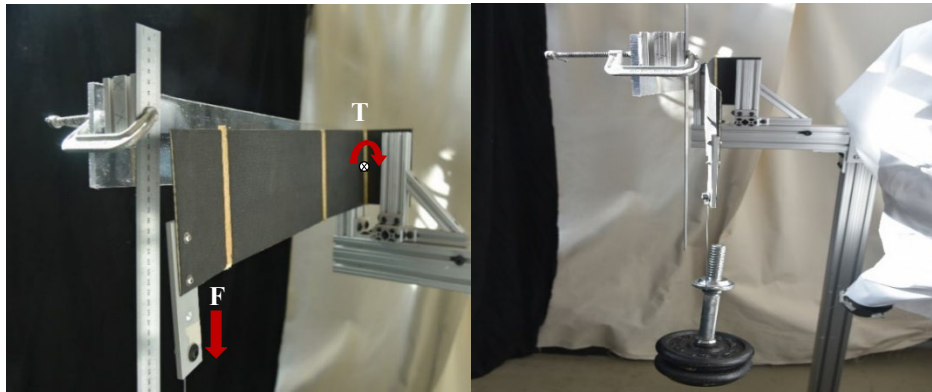


Fig. 9 Experimental setup for multihinge offset bend test

Table 5 Weight identification

Plate identification	Load N (lb)
Bar	18.00 (4.05)
A	12.25 (2.75)
B	13.35 (3.00)
C	21.13 (4.75)
D	22.25 (5.00)
E	37.81 (8.50)
F	111.21 (25.00)

Table 6 Weight selections for multihinge offset bend test

Trial	Plate identification	Load N (lb)
1	Bar + Plate D	40.26 (9.05)
2	Bar + Plate B, D	53.60 (12.05)
3	Bar + Plate A,B,D	65.83 (14.80)
4	Bar + Plate A, B, C, D	86.96 (19.55)
5	Bar + Plate C, D, E	100.31 (22.55)
6	Bar + Plate F	129.22 (29.05)

3. Results

3.1 Single-Hinge Offset Bend Test

The plots of the offset bend test's torque versus angle of twist for Designs 1–4 and the carbon–Al hinge are presented in Fig. 10. The yield strength of the Al hinge was reached during the first cycle; thus, only one cycle is shown. Each of Designs 1–4 exhibited some degree of nonlinearity across each cycle. For Designs 1, 2, and 3, Cycles 2–5 exhibit a noticeable deviation from Cycle 1, more so in the higher deflection angles. This deviation in mechanical behavior from Cycle 1 to Cycles 2–5 is most likely due to the propagation of delamination from the shearing effect that occurs during the first exposure to torsional loading. Notice no sudden drops in torque were recorded. Cycles 2–5 show good repeatability of mechanical behavior. The force threshold for each design case at 25.4 mm of displacement is shown in Fig. 11.

The torsional stiffness was evaluated as a linear fit to the initial slope ranging from 0 rad to 0.05 rad. This is presented in Fig. 12 and Table 7 along with a comparison of the numerical analysis from CLT. For application to the Third Arm exoskeleton prototype, it is desirable to limit the amount of vertical deflection.

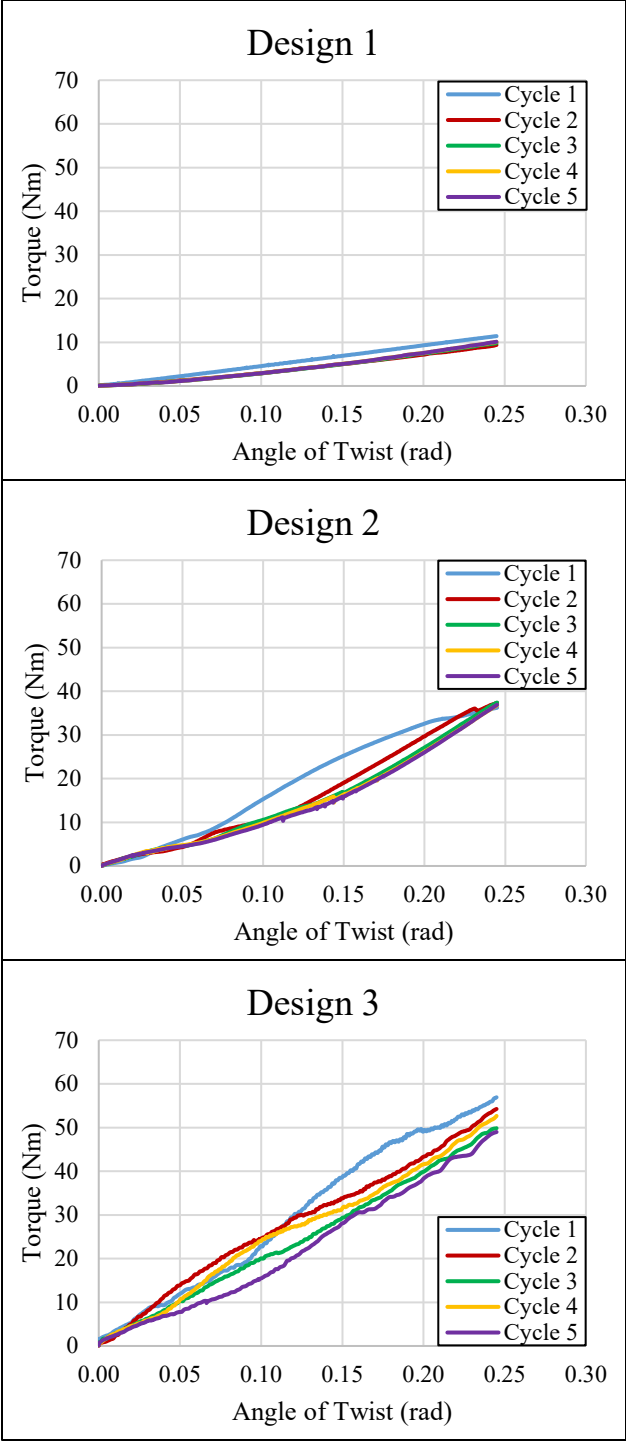


Fig. 10 Torque vs. twist plots from offset bend test

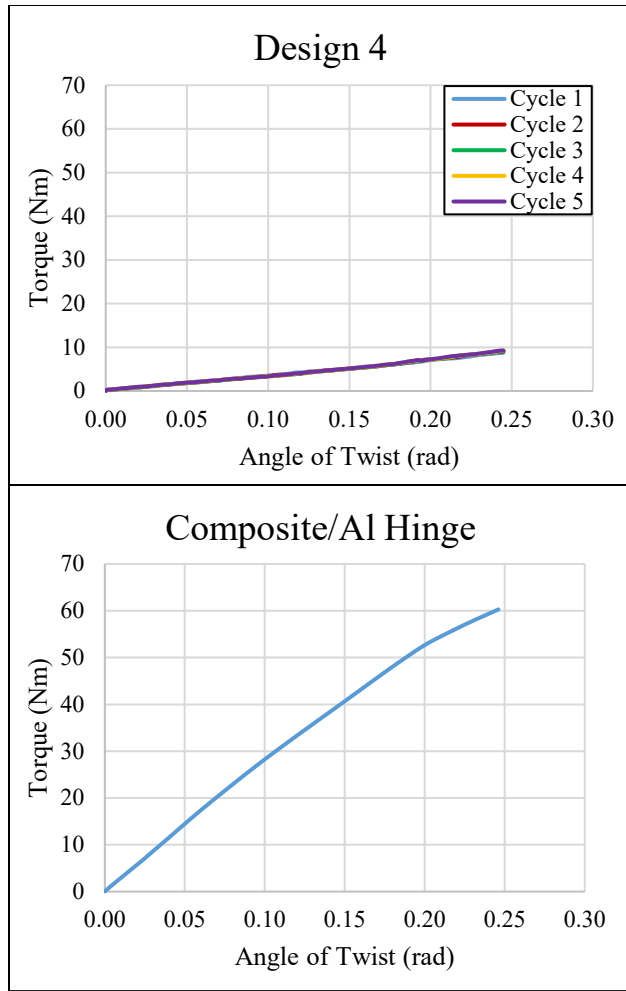


Fig. 10 Torque vs. twist plots from offset bend test (continued)

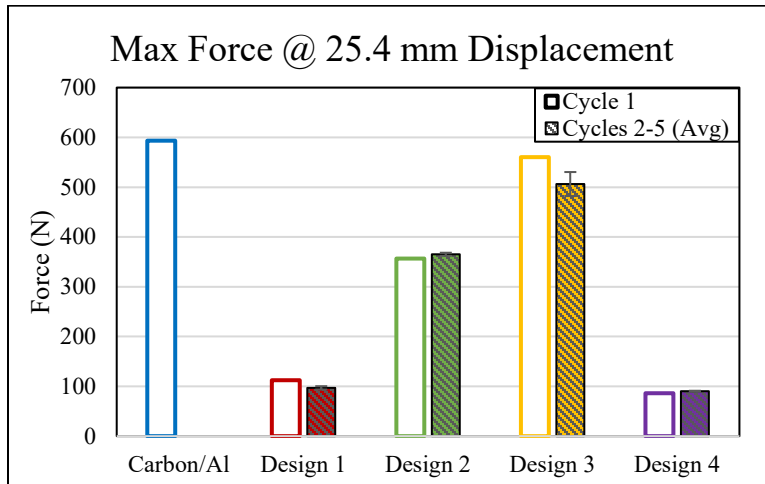


Fig. 11 Average force threshold for each design

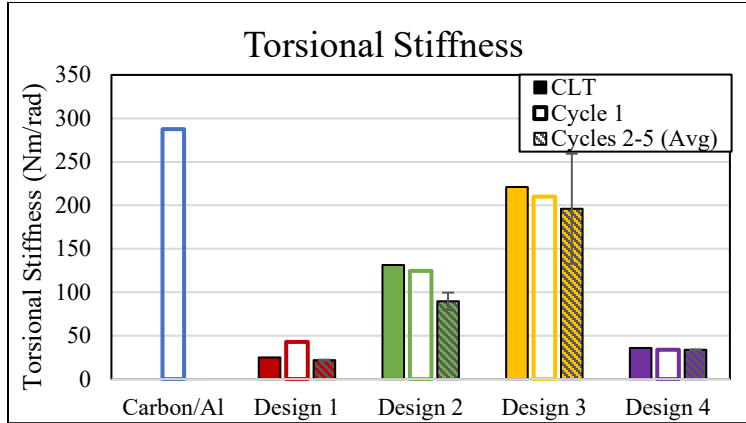


Fig. 12 Average torsional stiffness for each design

Table 7 Torsional stiffness for Designs 1–4 and Third Arm

Design	Hinge configuration	Torsional stiffness (Nm/rad)		
		Cycle 1	Cycles 2–5	% reduction
1	Kevlar, 1 ply, 152.4 mm wide, [$\pm 45^\circ$]	42.83	21.84	49.00
2	Kevlar, 2 ply, 152.4 mm wide, [$\pm 45^\circ$]	124.52	89.58	28.06
3	Kevlar, 3 ply, 152.4 mm wide, [$\pm 45^\circ$]	209.94	196.02	6.63
4	Kevlar, 2 ply, 76.2 mm wide, [$\pm 45^\circ$]	33.81	33.79	0.24
Carbon–Al	Aluminum 6061-T6	287.60	NA	NA

The experimental and numerical model values for torsional stiffness are in good agreement for Cycle 1 with the exception of Design 1. The out-of-plane to in-plane shear-modulus ratio, $G_{xz}:G_{xy}$, is 0.01:1 for Designs 1 and 4 and 0.005:1 for Designs 2 and 3, due to the influence the ratio of width to thickness has on $G_{xz}:G_{xy}$. However, Design 1 has a significantly higher width–thickness ratio (102:1) compared with Design 4 (33:1). This suggests the numerical approximation of $G_{xz}:G_{xy}$ being 0.01:1 underestimates the torsional stiffness properties for high ratios of width and thickness.

The variation in the force threshold between each cycle is relatively small across all designs. At high angular deformation, the Al hinge has a one-time use as plastic deformation occurs, as shown in the top row of images in Fig. 13. For the composite hinges (bottom row), there is a reduction in stiffness after the first cycle (as shown in Table 7 and Fig. 12). The single-ply hinge of Design 1 has the highest reduction of 49% followed by Design 2 with a reduction of 28%. Designs 3 and 4 have a marginal reduction in torsional stiffness after Cycle 1. In all designs, Cycles 2–5 exhibit good repeatability in force-deflection behavior and torsional stiffness. During and after testing there was no observed damage on the composite hinges,

besides what occurred during the initial 90° bending to fit into the fixture. The effects of composite-hinge ply count and width on average torsional stiffness across Cycles 2–5 are as follows. Comparing Designs 1 and 2, doubling the ply count results in a 4.1× improvement in stiffness. The 3-ply Design 3 demonstrates 9× higher stiffness than Design 1 and 2.2× higher than Design 2. Lastly, the effect of reducing the width in half from Designs 2–4 led to a 2.7× reduction in torsional stiffness. Although none of the composite-hinge designs exceeded the torsional stiffness of the carbon–Al hinge, the constituent properties of the composite hinge can be tailored to achieve a desired stiffness. However, for the particular application of interfacing a composite hinge with the Third Arm, there is a trade-off between torsional stiffness and pliable out-of-plane bending. As reported by Rowbottom et al.,¹ a 3-ply hinge design results in a relatively high out-of-plane bending stiffness. Therefore, an increase in ply count should not be considered for the application of the Third Arm. The experimental data demonstrates that, with the exception of Design 3, the force threshold at 25.4-mm displacement and the initial torsional stiffness for each design case are considerably lower than the carbon–Al hinge. Design 3 was also the only composite hinge able to withstand the minimum design torque load of 37 Nm. Thus, three Kevlar plies were chosen for the multihinge composite design.

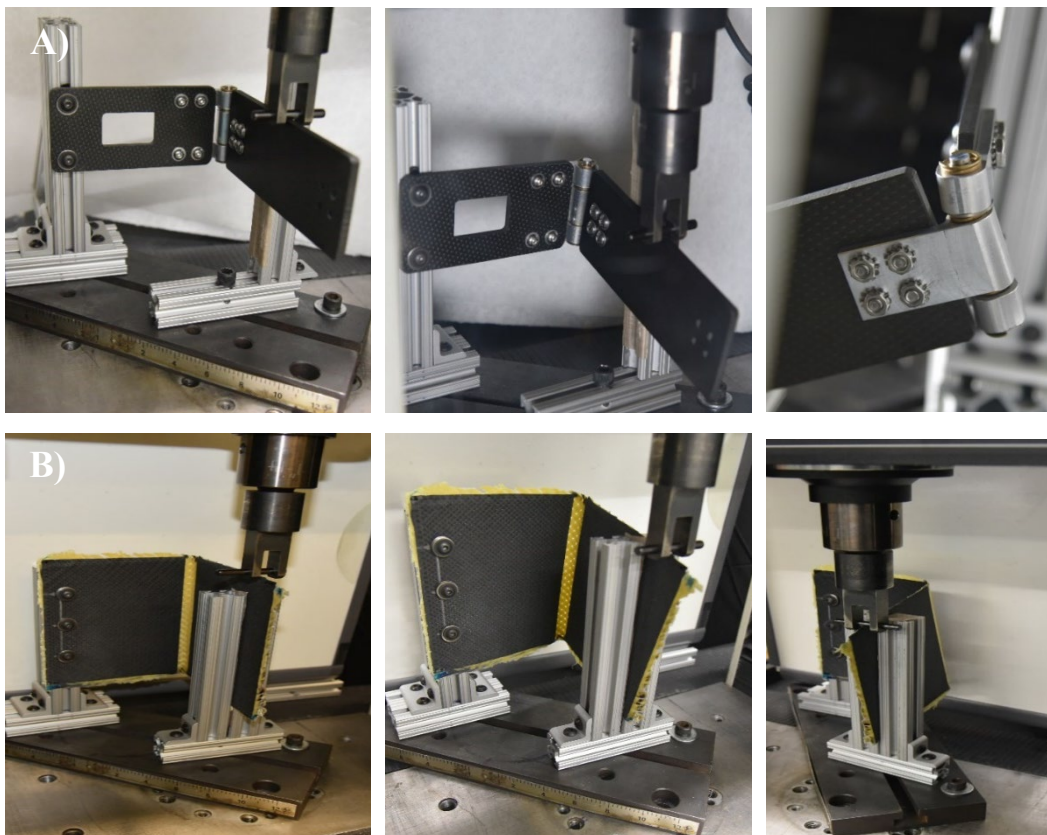


Fig. 13 Offset bend test's progression for a) carbon–Al hinge and b) composite hinge

3.2 Multihinge Offset Bend Test

The force-deflection and torsional behaviors for the two multihinge design variations are presented in Fig. 14. Each design case underwent the same loading conditions as presented in Table 6; however, only Design 6 went through Trial 6. Figures 15 and 16 show a visual comparison of the experimental testing that was conducted on Trial 5 for Designs 5 and 6. From the experimental data, significant vertical tip deflection occurred in Design 5, resulting in 48-mm deflection with Trial 1 alone and 118 mm for Trial 5. In addition, shown in Fig. 15, significant angular deformation occurred in the rear, rigid, carbon section that was pinned to the test fixture. As discussed in Section 2.1, carbon plies were added to the rigid sections of Design 6 to improve the torsional stiffness behavior in the rear panel and to limit the vertical tip deflection. The Kevlar hinge's length and ply count did not change between Designs 5 and 6. Despite having a reduced width compared with Design 5, the added carbon plies of Design 6 resulted in an average 28% reduction in vertical tip deflection compared with Design 5. Design 6 was also able to handle a 30% increase in maximum load (Trial 6) without failure.

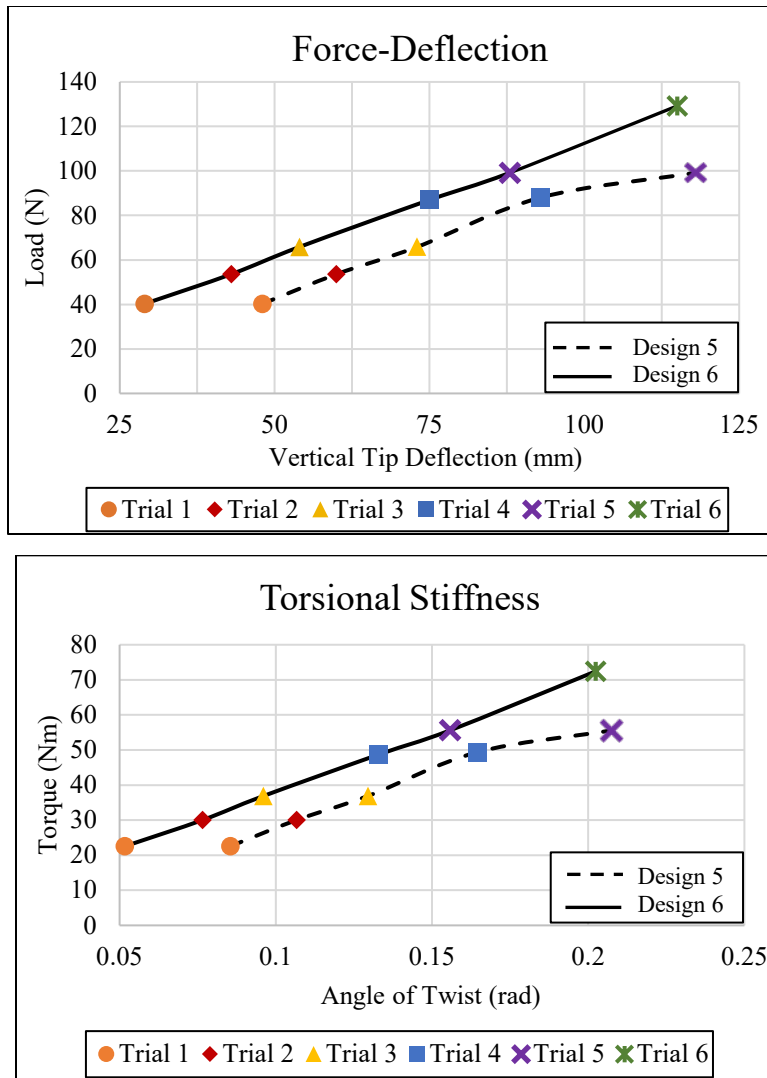


Fig. 14 Multihinge composite offset bend test's results

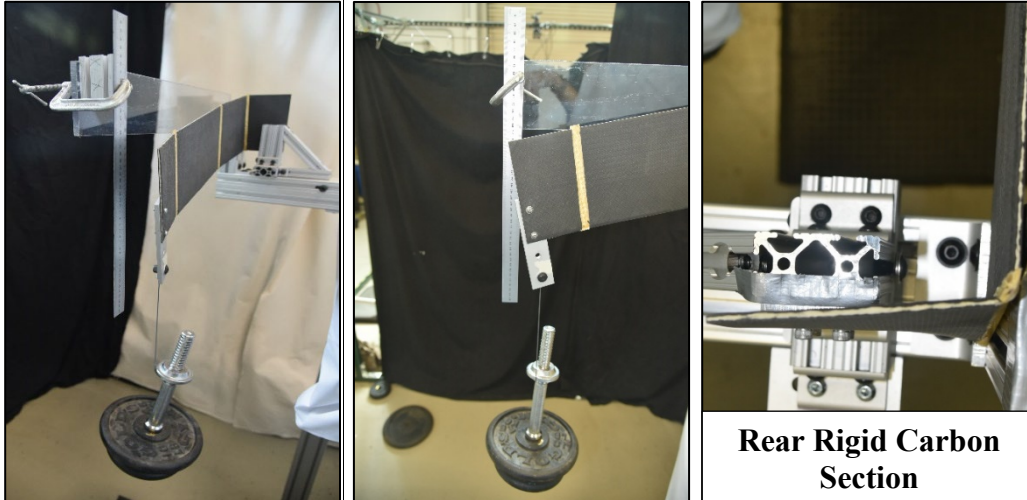


Fig. 15 Multihinge offset bend test, force-deflection behavior of Trial 5 of Design 5

Figure 16 illustrates the significant improvement in the torsional stiffness in the rear, rigid, carbon section. There is no visible angular deformation occurring in the rear rigid panel; however, significant angular deformation is still present within the hinge region, resulting in tens of millimeters of vertical tip deflection. Torsional stiffness was calculated as a linear fit of T/θ data for Trials 1–4. Design 5 stiffness was 336.5 Nm/rad, and Design 6 stiffness was 323.8 Nm/rad. From the results mentioned in Section 3.1, reduction in width significantly reduces composite torsional stiffness. However, the multihinge test’s results demonstrated the ability to maintain torsional stiffness despite the reduction in composite width through increase in ply count in the rear, rigid, carbon section. This will allow for future tailorability to achieve a more compact design for interfacing with the Third Arm. The only damage observed in Designs 5 and 6 was delamination between the Kevlar–PU in the rearmost hinge region. This damage was caused by the initial bending of the hinge to a 90° angle to fit into the test fixture. No additional damage was observed after testing.

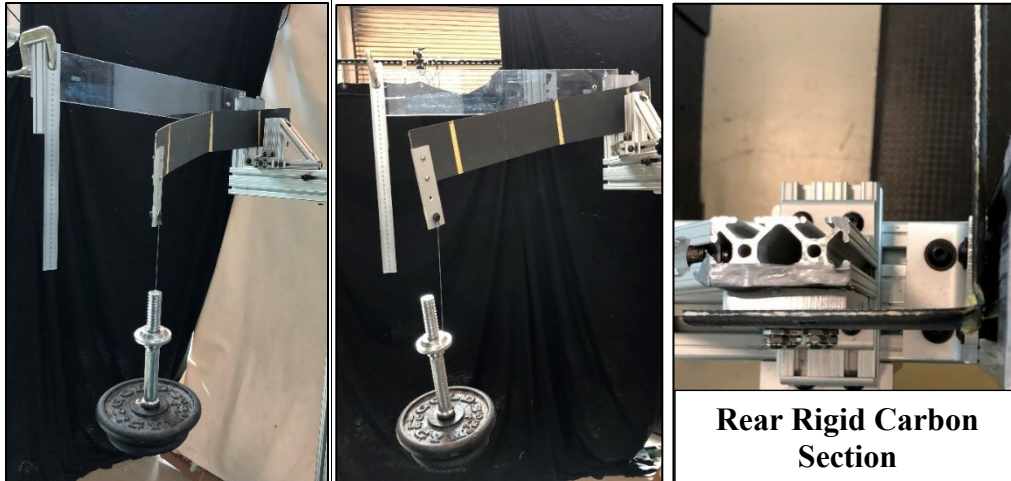


Fig. 16 Multihinge offset bend test, force-deflection behavior of Trial 5 of Design 6

3.3 Exoskeletal Application

After verifying the capability of the multihinge composite panel to withstand various loading conditions, it was then integrated into the Third Arm exoskeleton prototype as a demonstration platform. The existing series of carbon-laminate plates and aluminum hinges were replaced by the continuous multihinge composite as shown in Fig. 17. The image on top depicts a Soldier using an M4 carbine, weighing approximately 3.2 kg (7.2 lb). From experimental testing, the multihinge composites demonstrated the capability to hold the load of an M4 carbine. Design 6 was interfaced with the Third Arm prototype as shown in Fig. 17. Replacement of the existing series of carbon–Al hinge segments on the Third Arm with a continuous multihinge composite panel reduces the number of parts, assembly time, and overall mass. Table 8 lists the mass of each of the components. Retrofitting the Third Arm with the multihinge panel resulted in a substantial reduction in mass of 50% for Design 6 with approximately the same system performance for the M4 application. The multihinge composites are stiffer in out-of-plane flexion than the free-rotating Al hinges due to the 3-ply Kevlar composite and the epoxy that likely seeped into the hinge region.¹



Fig. 17 Integration of multihinge composite panel into Third Arm

Table 8 Comparison of masses of Third Arm and replacement multihinge composite panel

Components	Third Arm (g)	Design 6 (g)	Design 6 Reduction (%)
Composite	238.6	372.6	56.2
Al	373.7	0.0	100.0
Steel hardware	145.7	9.2	93.7
Total	758.0	381.8	49.6

4. Conclusion

This report demonstrated a method for manufacturing continuous fiber woven composites with multiple alternating regions of rigid (epoxy) and flexible (PU) segments. A novel testing method was designed to analyze the torsional stiffness behavior in an offset bend test, where the composite hinge was bent to 90° and

subjected to a vertical load. Numerical modeling through CLT accurately predicted the torsional stiffness behavior of multi-ply hinged composites, but underestimated the stiffness for a single-ply hinge. This was due to the model being dependent on width-to-thickness ratio and the ratio of in-plane to out-of-plane shear modulus. For comparison, the force threshold and torsional stiffness for the carbon–Al hinge off the Third Arm and the composite-hinge designs (single-hinge segment) were evaluated for low-cycle loading. After the first cycle, the Al hinge from the Third Arm exhibited plastic deformation, whereas the composite-hinge design cases demonstrated only relatively small changes in stiffness. The tailorability of the torsional stiffness for single-hinge composites guided the design process for multihinged composite panels. The multihinged composite panels were evaluated through the offset bend test and demonstrated significant vertical tip deflection under loading. Changes in the constituent properties of the multihinge composite significantly reduced the tip deflection as well as being able to take on higher loads. The ability to predict, design, and characterize torsional stiffness of these composites allowed for interfacing the continuous multihinged composite panel into the Third Arm exoskeleton prototype, thus reducing the segment weight by 50% and reducing complexity of the exoskeleton.

Future work: Improvements to the manufacturing method could prevent epoxy from seeping into the tows of the flexible-hinge section, thus improving the out-of-plane flexibility of the Kevlar hinge sections. A liquid PU could be infused into the entire area of the flexible fabric layer or layers, then the flexible section could be masked while epoxy resin is infused into the rigid fabrics flanking the flexible region. This manufacturing method may also allow for improved torsional stiffness through reduction in the flexible region's length. Chemical pretreatment of the Kevlar fabric or selection of Kevlar fabric and TPU matrix with known compatibility could improve adhesion of the Kevlar and TPU, potentially reducing damage and increasing torsional strength. Additional carbon plies and/or novel laminate-plate geometries will allow for further reduction in overall composite width and vertical tip deflection of the multihinged composite, enabling a more compact structure and better usability for heavier loads on the Third Arm.

5. References

1. Rowbottom C, Moore LA, Baechle DM. Composite living hinges for robotic applications. Aberdeen Proving Ground (MD): CCDC Army Research Laboratory (US); 2020 Sep. Report No.: ARL-TR-9016.
2. Maqueda Jiménez I. High strain composites and dual-matrix composite structures [dissertation]. [Pasadena (CA)]: California Institute of Technology; 2014.
3. López JF, Pellegrino S. Folding of fiber composites with a hyperelastic matrix. *Int J Sol Struc*. 2013;49(3–4):395–407.
4. Platt DL. Tailoring the bending stiffness of elastomeric dual-matrix composites [master's thesis]. [Toronto, Canada]: University of Toronto; 2016.
5. Carbon–Kevlar hinge. Sydney (Australia): Talon Technology; c2017 [accessed 2020 May]. <https://www.carbonhinge.com>.
6. Lacdan J. Army researchers advance ‘Third Arm’ project to next testing phase. *Army News Service*; 2018 Mar 1 [accessed 2020 May]. https://www.army.mil/article/201229/army_researchers_advance_third_arm_project_to_next_testing_phase.
7. Sumsion HT, Rajapakse YDS. Simple torsion test for determining the shear moduli of orthotropic composites. In: Noton BR, editor. *Proceedings of the 1978 International Conference on Composite Materials*; 1978 Apr 16–20; Toronto, Canada. Warrendale (PA): Metallurgical Society of AIME; c1978. p. 994–1002.
8. Tsai CL, Daniel IM. Determination of in-plane and out-of-plane shear moduli of composite materials. *Exp Mech*. 1990;30:295–299.
9. Davalos JF, Qiao P, Wang J, Salim HA, Schlussek J. Shear moduli of structural composites from torsion tests. *J Comp Mat*. 2002;36:1151–1173.

List of Symbols, Abbreviations, and Acronyms

2-D	two-dimensional
Al	aluminum
ARL	Army Research Laboratory
CCDC	US Army Combat Capabilities Development Command
CLT	Classical Laminate Theory
DOF	degree of freedom
L	length
NA	not applicable
PTFE	polytetrafluoroethylene
PU	polyurethane
T	thickness
VARTM	vacuum-assisted resin transfer molding
W	width

1 DEFENSE TECHNICAL
(PDF) INFORMATION CTR
DTIC OCA

1 CCDC ARL
(PDF) FCDD RLD DCI
TECH LIB

2 CCDC ARL
(PDF) FCDD RLW MA
C ROWBOTTOM
D BAECHLE